

A Brazil Basin Reprise

Kurt L. Polzin *

Abstract

The intent of this note is to discuss the information content and interpretation of data obtained during the Brazil Basin Tracer Release Experiment (BBTRE). Two geologic features of the Mid-Atlantic Ridge figure prominently in this work: abyssal hills and offset fractures. Abyssal hills dominate the topographic slope variance and therefore are central in internal tide generation and internal wave scattering issues. Offset fractures are important as they serve as conduits for deep flow from mid-basin to ridge crest. The Smith-Sandwell satellite altimetry derived topography is a band-passed representation of topographic variability and does not resolve horizontal wavelengths smaller than 20-30 km. It does not resolve the topographic slope or curvature of abyssal hills. Attempts by St.Laurent et al. (2001) and Thurnherr et al. (2005) to bin average vertical profiles based upon point wise estimates of topographic slope and curvature in the Smith-Sandwell data set as offset fracture valleys, the sloping sides of offset fractures and adjacent regions are not supported by shipboard data products. Consequently Thurnherr et al. (2005)'s assertion that mixing over the sloping sides of the offset fractures exceeds that over adjacent regions is not supported by the observations.

Sediment collects preferentially in the depths of the offset fractures. Thus the fracture valley floors are significantly smoother than adjacent regions and moored data collected within a fracture valley as part of the BBTRE may not document the same internal wave environment as above regions removed from the fracture valley floors. Consideration of internal tide ray trajectories suggests that only the shallowest BBTRE current meters are representative of tide-topography interactions outside the fracture valleys. Thurnherr et al. (2005) note that subinertial energy deep within the offset fracture valleys exceeds the internal wave band energy and this observation is used to rationalize larger dissipation rates on the offset fracture sidewalls. However, Thurnherr et al. (2005)'s assumption that the moored data document the internal wave climate above the sloping sidewalls is not supported by linear wave kinematics.

Thurnherr et al. (2005) note the proximity of an offset fracture profile having the largest dissipation rates to a narrow sill cutting across the offset fracture and view the correspondence as being suggestive of a cause and effect relationship between the sill and the heightened dissipation. However, the spatial polarization of that station's velocity profile is inconsistent with the finestructure being associated with sill flows.

Taken collectively, there is no evidence to support the contention of Thurnherr et al. (2005) that sills processes are responsible for the bulk of the observed diapycnal mixing in the Brazil Basin.

1. Introduction

A basic description of the spatial variability of turbulent mixing in the Brazil Basin based upon the first of two cruises was presented in Polzin et al. (1997). In that paper we argued that enhanced mixing and turbulent dissipation above the Mid-Atlantic Ridge were associated with internal waves, proposed that the energy source for the internal wavefield was barotropic tides impinging on the rough bathymetry of the ridge and emphasized that the small scale structure of the ocean bottom appears to be key. This latter issue is pursued quantitatively in Polzin (2004).

Two features of mid-ocean ridges are of particular importance: abyssal hills and offset fractures. The Mid-Atlantic Ridge is cut by offset fractures, which are evident as rectilinear canyons running normal to the ridge crest and extending across much of the basin. Offset fracture valleys serve as conduits for deep flow from mid-basin to ridge crest, (Thurnherr et al. 2005). The Mid-Atlantic Ridge is also textured with abyssal hills. Abyssal hills are anisotropic and asymmetric features and are understood to be formed by faulting and volcanism at the ridge crest. Their morphology is believed to depend upon basin-scale attributes of ridge processes such as spreading rates and elastic thickness of the lithosphere adjacent to the ridge axis, e.g., Goff (1991). Rms heights of 200 m and a distance between peaks of 6–10 km are typical of the Mid-Atlantic Ridge. The topographic slope and curvature variance are dominated by abyssal hills. As opposed to being isolated like offset fractures, abyssal hills are ubiquitous features, filling in the areas in between the offset fractures. Abyssal hills are not well-represented in global topographic data sets [e.g., GEBCO, ETOPO, or Smith and Sandwell (1997)] as a multi-beam echosounding system is required to map such small scales and multi-beam coverage of the world's ocean is spotty (Becker and Sandwell 2006).

Significant effort was expended in Polzin (2004) in quantitatively linking the 6-10 km wavelength abyssal hills to corresponding vertical wavelengths through internal wave kinematics, assigning an amplitude to that wavefield by using an internal tide generation model and then estimating the turbulence associated with that wavefield by invoking ideas of nonlinearity and wave breaking. The evolution of that internal wave spectrum and turbulent dissipation with height above bottom was estimated using a radiation balance scheme. Internal wave shear spectra are peaked and decay with increasing height above boundary. That decay is sensibly consistent with the observed decay of turbulent dissipation with increasing height above boundary being a result of nonlinearity and internal wave breaking.

There is room for improvement, however. First, the generation model tends to assign a smaller vertical scale to the shear spectral peak than is observed. That peak was interpreted as representing a transition from the linear to advective limits in the generation problem, in which the energy density of the internal tide changes from being proportional to the topographic slope spectrum to proportional to the topographic height spectrum. A possible reconciliation is that the scattering of the internal tide should be viewed as simply reinforcing the barotropic tidal amplitude so that the peak in the shear spectrum appears at larger vertical wavelengths. Second, there are indications of excess horizontal kinetic energy in the vertical wavenumber spectra at large vertical wavelengths. Third, the idealized solutions addressed in Polzin (2004) assign a single expected value for internal wave frequency to interpret the spectra and dissipation profiles. A better pattern match to the observations would be obtained if a lower frequency (lower than semidiurnal) was used. Both these second and third issues could be addressed by considering the contribution of a near-inertial field to the observed spectra. This would presumably result from the parametric subharmonic decay of the tide. Inclusion of such a decay was beyond the scope of the nonlinear closure introduced in Polzin (2004) for the purpose of studying

the near-boundary decay process in a more strongly interacting wavefield. A complication in Polzin (2004) is that the conductivity cell of the High Resolution Profiler's CTD was broken for approximately half of the profiles being analyzed. There consequently was no independent estimate of wave frequency from the ratio of kinetic to potential energy.

In Ledwell et al. (2000) we recognized that the High Resolution Profiler data are biased. The bias results in part from sampling across spatial and temporal trends in the underlying physical variables associated with an internal tide generation problem: spatial gradients in the barotropic tidal amplitude, a fortnightly modulation of the tidal amplitude, spatial gradients in stratification and variability in the underlying topography. The sampling strategy also contributed to the biasing issue: a priority in tracer sampling was to obtain tracer free samples from beneath the target isopycnal and this led to most of the profiles being obtained within canyons or distinct depressions apparent in the Smith-Sandwell topography. In choosing station locations a concerted effort was made to avoid possible sills cutting across canyons. A third possible bias issue is that it proved to be difficult to reliably terminate the HRP profile above steep slopes, especially for isolated stations. The peaks and troughs of abyssal hills were thus targeted rather than their sloping sides.

The biasing issues can be interconnected and problematic. During the first cruise a series of stations were occupied between 16-18°W along a ridge to the north of the injection site. The near-bottom stratification for these stations is typically higher than the rest of the data set, and efforts at characterizing the near-bottom dissipation associated with the internal tide generation problem would lead me to predict, all things being equal, that these stations would have higher near boundary dissipations and the dissipation profile would exhibit greater bottom trapping. However, those stations were occupied over a period of 3.5 days during neap tide conditions in which the barotropic tide is at a minimum. A set of stations was occupied along and adjacent to the rift valley between 11 and 14° W during spring tide conditions during the second cruise. Detailed bathymetry is required to interpret these data. Reconstructing the bathymetry from the (single beam) onboard record for these stations has been problematic. A definitive interpretation of these spatial survey data is unlikely.

Our initial investigation (Polzin et al. 1997) raised a very interesting question about the mass budget of the abyssal Brazil Basin. In a diapycnal advection-diffusion balance

$$w^* = -\frac{\rho_o}{g} \frac{\partial \Gamma \epsilon}{\partial \rho} \cong N^{-2} \frac{\partial \Gamma \epsilon}{\partial z} \quad (1)$$

with diapycnal velocity w^* , density ρ and gravitational constant g in which the turbulent buoyancy flux has been related to the rate of dissipation of turbulent kinetic energy ϵ through an efficiency factor Γ , the sign of w^* is given by the sign of $\partial_z \epsilon$ if Γ is assumed to be constant. The dramatic enhancement of ϵ above rough topography implies downwelling and we hypothesized that the mass budget would be closed by upwelling within the canyons rather than above rough topography or the much smoother western half of the basin. We forwarded the conjecture that, on a broad scale, the Mid-Atlantic Ridge could be viewed as a permeable, sloping boundary with sinks for the densest waters in the Brazil Basin at the depths of the canyon mouths and sources of water at depths about the canyon heads. Unstated was the back of the envelope calculation implying substantial flow up the offset fractures: the requirement of laundering 2×10^6 m³ s⁻¹ of dense water through some 30 canyons in the abyssal Brazil Basin having a characteristic cross-sectional area $\frac{1}{2}HW$ with height $H = 700$ m and width $W = 20,000$ m returns an average velocity of 0.02 m s⁻¹. Additional funding was obtained to deploy a mooring in the offset fracture with the primary goal of documenting such a mean flow and the secondary goal

of documenting temporal characteristics of the internal wavefield. The back-of-the-envelope calculation is in remarkable agreement with two-year averaged estimates of flow in the canyon (Thurnherr et al. 2005).

In positioning the mooring I used the Smith-Sandwell bathymetry to select a site with relatively contiguous northern and southern walls and a relatively flat bottom. The later criterion was invoked as I intended the upper, more closely spaced, current meters to be *above* the depth at which semi-diurnal ray trajectories emanating from the northern and southern canyon walls would intersect. I made this choice as the HRP data indicated that turbulent dissipation profiles obtained within canyon bottoms were not as strongly enhanced with depth as profiles obtained above rough topography and I was attributing this to differences in the internal tide generation problem.

2. Commentary

More recently, Thurnherr et al. (2005) claim that mixing associated with subinertial flow over sills within and on the sloping sides of offset fracture canyons dominates that associated with internal tides. They present a variety of circumstantial evidence: (i) Horizontal density gradients being greatest in the vicinity of sills (extensions of abyssal hill crests) cutting across the canyons, (ii) current meter records indicating subinertial variance dominating tidal variance at a level 600 m above the canyon floor, (iii) Average 'crest', 'slope' and 'valley' dissipation profiles presented in St.Laurent et al. (2001) suggesting that dissipation was weakest and least depth enhanced for 'crest' profiles, with the implication that the 'crest' profiles are representative of a relatively weak internal tide process, and (iv) the proximity of a station having large dissipation rates to a canyon sills.

I have examined these claims in detail and find that the data, apart from issue (i), do not support their interpretation.

a. Binning with Smith-Sandwell

The average 'crest', 'slope' and 'valley' profiles presented in St.Laurent et al. (2001) were binned using an algorithm based upon topographic slope and curvature estimates from the Smith-Sandwell bathymetry data set (Smith and Sandwell 1997). The binning of these profiles evidently was not ground-truthed against shipboard bathymetric data products: their crest profile is inconsistent with data presented in Fig. 3 of Polzin et al. (1997), for which the corresponding dissipation profiles appear in Fig. 1, in which it is apparent that the 'crest' dissipations are largest and most depth enhanced. In question is a grouping of seven profiles at the 21°32.5'S station. The binning of these seven profiles is significant as they will dominate an average. The characterization of these seven profiles as 'crest' stations is unambiguous when the Smith-Sandwell Fig. 2 and multi-beam bathymetry are compared, Fig. 3. See as well the bathymetry in Fig. 1

In my work I have binned data simply with respect to the presence or absence of abyssal hills and used profiles from the first cruise which I believe are representative of abyssal hill regimes. I have averaged the northern most five stations in Figs 1 with other data obtained to the east along the ridge crest during the first Brazil Basin cruise (Fig. 2 & 3) to arrive at the curve in Fig. 4 and used in Polzin (2004). Including data from the second cruise in this 'abyssal hill' average is unlikely to produce the 'crest' curve appearing in St.Laurent et al. (2001), Fig. 5. Quantitative impacts on the zonal overturning estimates produced in St.Laurent et al. (2001) are

likely.

b. Interpreting Moored Data

The second issue is interpreting the information content of the moored data relative to internal tide generation and internal wave scattering processes above rough topography. The mooring was placed in a relatively flat canyon bottom, Fig. 6. Information about the character of the bottom is carried along internal wave ray trajectories and the transmitted information is that of the kinematic bottom boundary condition of no normal flow as represented in the internal tide generation and internal wave scattering problems - minus the information lost due to nonlinearity. Toole (2007) remarks that the bottom most current meters - those at 5023, 4878, 4660 and 4635 m with anchor at 5115 m water depth - contain information at tidal frequencies of the relatively flat canyon bottom. Current meters at 4005, 3980, 2959 and 2934 m water depth contain information at tidal frequencies about rough topography on the sloping walls of the offset fractures. The information content is that, in the linear wave, infinitesimal amplitude topography limit, the vertical wavenumber internal wave energy density is proportional to the horizontal wavenumber topographic *slope* spectral density, Polzin (2004).

In an attempt to be slightly more quantitative I have, in view of the two dimensional nature of the topography, considered the topographic slope variance¹ along circles about the mooring, Fig. 7. The radii of these circles corresponds to rays that intersect the current meters if those rays were to originate at the mooring anchor depth (5115 m). In order to account for variations of information associated with variations in stratification, I have buoyancy scaled the bottom topography according to:

$$z' = 4800 + \int_{4800}^{z^*} \frac{N(z)}{N_o} dz \quad (2)$$

with reference value $N_o = 1 \times 10^{-3} \text{ s}^{-1}$. I find that the buoyancy scaled topographic slope variance ($|\nabla z'|^2$) at the $z = 4600, 4000$ and 3000 m current meters is in the ratio 0.072:1.0:5.3.

I view Thurnherr et al. (2005)'s finding that subinertial energy dominates tidal energy at 4600 m as a confirmation that the offset fracture canyon floors are flat and that the current meter data at that level do not reveal information about the relative nature of subinertial versus tidal processes on the sidewalls of the offset fractures.

While ray trajectories originating from the sloping sidewalls of the offset fractures do intersect the 4000 m level at the mooring, it is evident that the preponderance of the information content is that of a relatively flat and weakly stratified offset fracture canyon. The internal wave climate documented by the mooring likely differs from that above rough topography.

c. Horizontal Polarization of a 'sill' station

Thurnherr et al. (2005) note that, of the HRP profiles obtained above the offset fracture floor during the second cruise (the white filled squares in Fig. 2), the one (# 23 at $14^\circ 30' \text{W}$) having the largest dissipation rates lies adjacent to a narrow sill cutting across the offset fracture valley. Thurnherr et al. (2005) view the correspondence as being suggestive of subinertial flow over the sill being the cause of the heightened dissipation.

¹The astute reader will note that the information content reaching the mooring is likely the topographic slope variance in the radial direction along the intersection of the ray trajectory with the actual bathymetry. I simply consider the total slope variance on the circle.

In the high frequency limit, the velocity trace of a single plane wave is rectilinearly polarized with horizontal velocity parallel to the horizontal wavevector with the horizontal wavevector being dictated by the topography. The deep velocity field of Station 23 is polarized in the cross-canyon direction, Fig. 8, inconsistent with generation by either subinertial or tidal flows impinging upon the sills.

3. Discussion

The buoyancy budget within the fracture zone valleys of some 0.02 m s^{-1} up-canyon flow across sloping isopycnals demands significant diapycnal transformations in combination with net upwelling. These transformations may very well be associated with sill processes such as those documented within the Romanche Fracture Zone, Ferron et al. (1998). However, I have not significantly changed my opinion put forward in (Polzin et al. 1997) about the importance of tides and the detailed character of the bathymetry for the interpretation of the HRP data. Those data are decidedly biased away from addressing the role of sills in the canyon's zonal overturning circulation.

The conundrum posed by the inference of downwelling above rough topography, i.e. averaging dissipation profiles in a height-above-bottom coordinate system and equating that coordinate in the context of a diapycnal advection-diffusion balance (1), is probably misleading. In Polzin (2008) I explore the consequences of averaging in a height above the *mean* boundary coordinate system and predict a diapycnal velocity estimate that is consistent with both tracer observations of downwelling and a basin scale mass budget that requires upwelling.

Acknowledgments.

Salary support for this analysis was provided by Woods Hole Oceanographic Institution bridge support funds.

References

- Becker, J. J. and D. T. Sandwell, 2006: Global estimates of seafloor slope from single-beam ship soundings. *J. Geophys. Res.*, **113**, doi:10.1029/2006JC003879.
- Ferron, B., H. Mercier, K. Speer, A. Gargett, and K. Polzin, 1998: Mixing in the romanche fracture zone. *J. Phys. Oceanogr.*, **28**, 1929–1945.
- Goff, J. A., 1991: A global and regional stochastic analysis of near-ridge abyssal hill morphology. *J. Geophys. Res.*, **96**, 21 713–21 737.
- Ledwell, J. R., E. T. Montgomery, K. L. Polzin, L. C. St.Laurent, R. W. Schmitt, and J. M. Toole, 2000: Evidence for enhanced mixing over rough topography in the abyssal ocean. *Nature*, **403**, 179–182.
- Polzin, K. L., 2004: Idealized solutions for the energy balance of the finescale internal wavefield. *J. Phys. Oceanogr.*, **34**, 231–246.
- , 2008: An abyssal recipe. *submitted to Ocean Modeling*.
- Polzin, K. L., J. M. Toole, J. R. Ledwell, and R. W. Schmitt, 1997: Spatial variability of turbulent mixing in the abyssal ocean. *Science*, **276**, 93–96.
- Smith, W. H. F. and D. T. Sandwell, 1997: Global seafloor topography from satellite altimetry and ship depth soundings. *Science*, **277**, 1956–1962.
- St.Laurent, L. C., J. M. Toole, and R. W. Schmitt, 2001: Buoyancy forcing by turbulence above rough topography in the abyssal brazil basin. *J. Phys. Oceanogr.*, **31**, 3476–3495.
- Thurnherr, A. M., L. C. St.Laurent, K. G. Speer, J. M. Toole, and J. R. Ledwell, 2005: Mixing associated with sills in a canyon on the midocean ridge flank. *J. Phys. Oceanogr.*, **35**, 1370–1381.
- Toole, J. M., 2007: Temporal characteristics of abyssal finescale motions above rough bathymetry. *J. Phys. Oceanogr.*, **35**, 409–427.

List of Figures

1	Profiles of average dissipation rate ϵ vs depth and latitude for a set of 6 stations during BBTRE1. Multibeam bathymetry is in black. Dissipation for the shallowest station is largest and most strongly depth enhanced. See Fig. 3 of Polzin et al. (1997) for corresponding depth profiles of diapycnal diffusivity. That figure used a depth contour estimated from single beam sensor data. From north to south there are (2, 2, 7, 4, 3, 4) profiles in each station. These 6 stations appear as the filled white circles along $18^\circ 30' W$ in Fig.s 2 and 3.	10
2	Station positions of High Resolution profiler dives. Circles represent profiles obtained in 1996, squares profiles obtained in 1997. White filled symbols represent profiles discussed in this work.	11
3	Smith-Sandwell (upper panel) and Multibeam (lower panel) bathymetry. 'Canyon' stations are represented by white-filled squares and the southern most white filled circle. The remaining white filled circles represent 'abyssal hill stations'. In question is the interpretation of the third station (from north to south) in Fig. 1 and in the multibeam map (lower panel) with regards to 'crest'-'slope'-'valley' or 'abyssal hill'-'canyon' characterizations. See Fig.s 2 and 7 for depth scales.	12
4	Profiles of average dissipation rate ϵ vs depth for 'canyon' (left panel) and 'abyssal hill' stations. Canyon stations are represented as white filled squares and the southern most white filled circle in Fig.s 2&3. Abyssal hill stations are represented by the other white filled circles. The profiles have been averaged in a height-above-bottom coordinate system over the bottom most 2000 m and in a depth coordinate system in the upper part of the water column. The extent of the vertical axis represents represents the mean depth.	13
5	Profiles of average dissipation rate ϵ vs depth for 'crest', 'valley' and 'slope' profiles, Figure from Ledwell et al. (2000), permission from <i>Nature</i> . See also Fig. 3 of St.Laurent et al. (2001).	14
6	Topography (black) along a line normal to the canyon axis. The origin marks the mooring position. Semidiurnal frequency rays intersecting individual current meters at nominal depths of 4600, 4000 and 3000 m are indicated. See also Fig. 2c of Toole (2007)	15
7	2-D multi-beam map indicating the origin of semidiurnal frequency rays passing through individual current meters. A cross marks the mooring location. Rings represent the locus of points passing through current meters at the indicated depths and originating at the depth of the mooring anchor. Upper panel: Observed bathymetry. Lower panel: Buoyancy scaled bathymetry.	16
8	Station 23 data (second Brazil Basin survey). Left panel: Dissipation. Right panel: Horizontal velocity rotated into across (thin line) and along (thick line) canyon coordinates. Variability in across-canyon velocity coincides with enhanced dissipation discussed by Thurnherr et al. (2005).	17

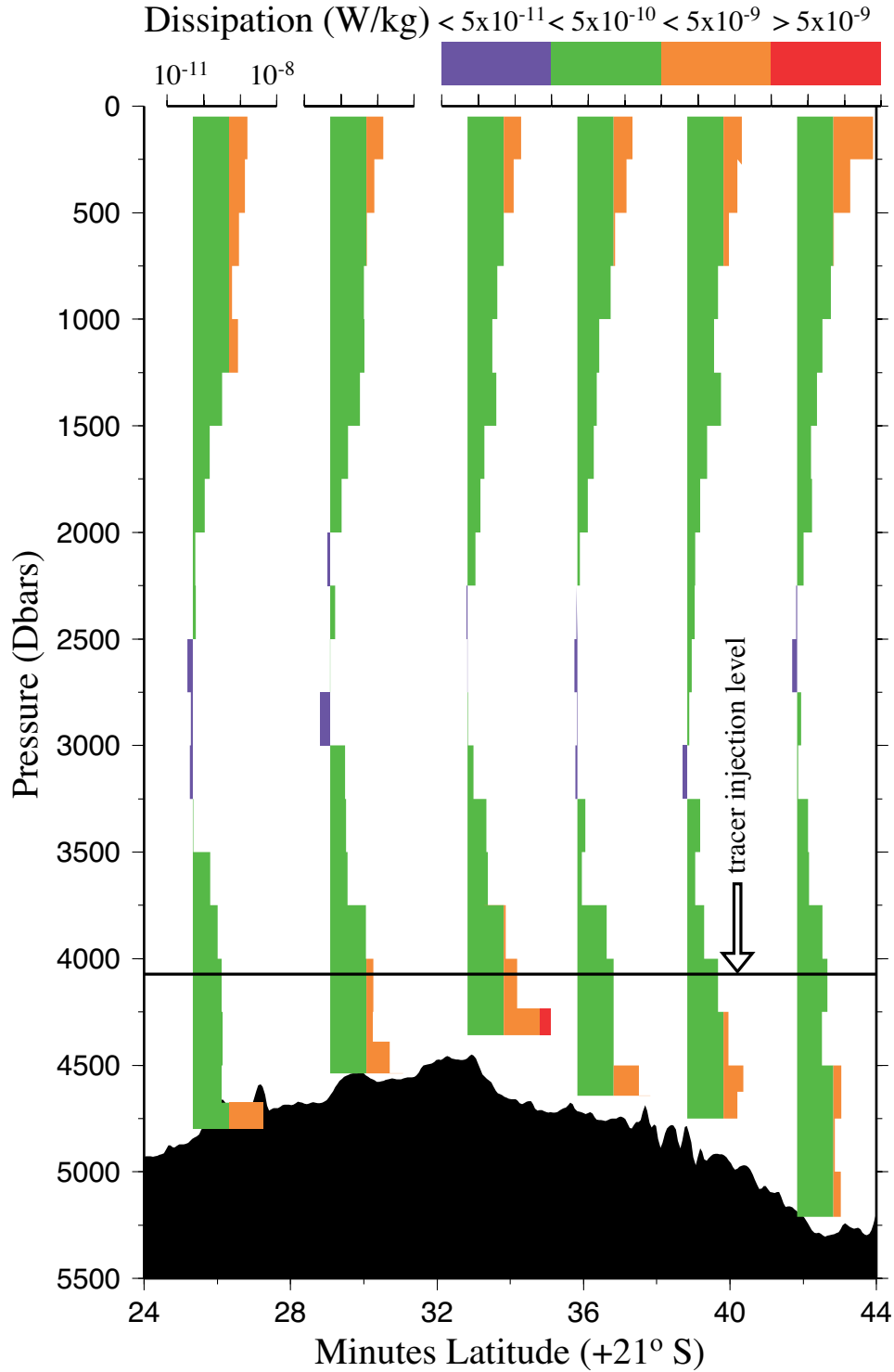


FIG. 1. Profiles of average dissipation rate ϵ vs depth and latitude for a set of 6 stations during BBTRE1. Multibeam bathymetry is in black. Dissipation for the shallowest station is largest and most strongly depth enhanced. See Fig. 3 of Polzin et al. (1997) for corresponding depth profiles of diapycnal diffusivity. That figure used a depth contour estimated from single beam sensor data. From north to south there are (2, 2, 7, 4, 3, 4) profiles in each station. These 6 stations appear as the filled white circles along $18^\circ 30' \text{ W}$ in Figs 2 and 3.

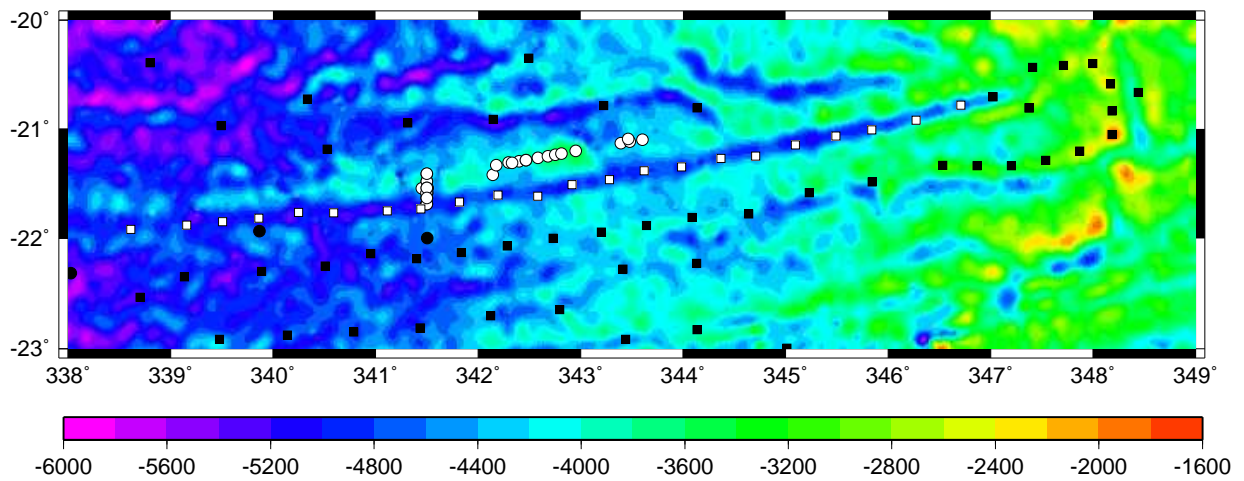


FIG. 2. Station positions of High Resolution profiler dives. Circles represent profiles obtained in 1996, squares profiles obtained in 1997. White filled symbols represent profiles discussed in this work.

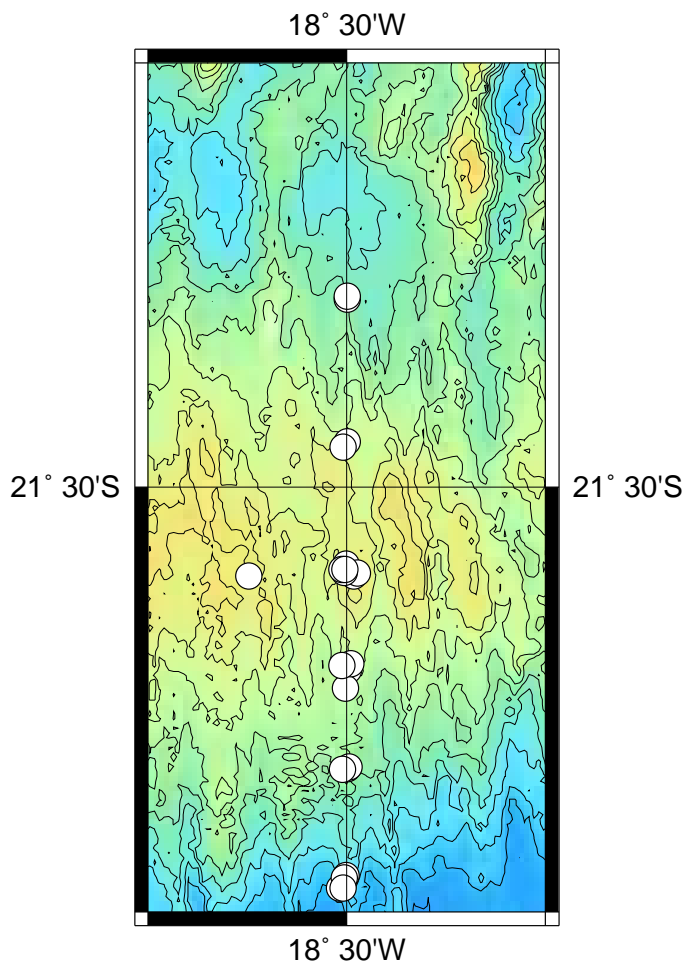
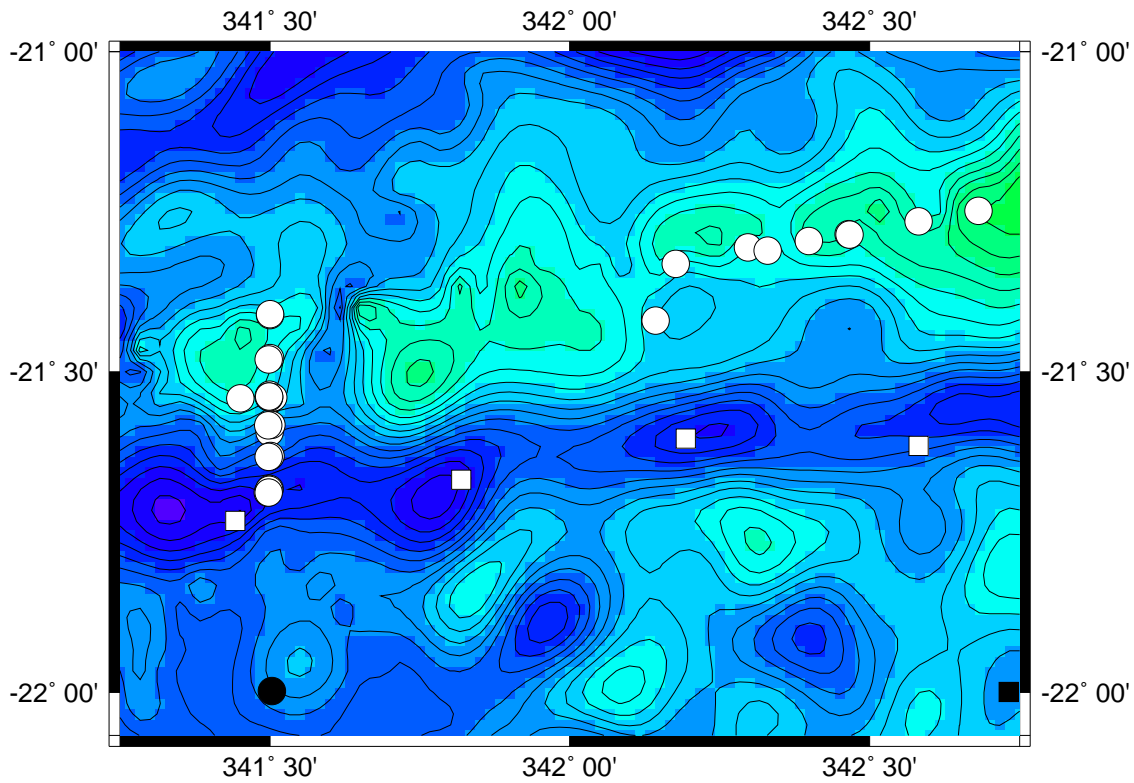


FIG. 3. Smith-Sandwell (upper panel) and Multibeam (lower panel) bathymetry. 'Canyon' stations are represented by white-filled squares and the southern most white filled circle. The remaining white filled circles represent 'abyssal hill stations'. In question is the interpretation of the third station (from north to south) in Fig. 1 and in the multi-beam map (lower panel) with regards to 'crest'-'slope'-'valley' or 'abyssal hill'-'canyon' characterizations. See Figs 2 and 7 for depth scales.

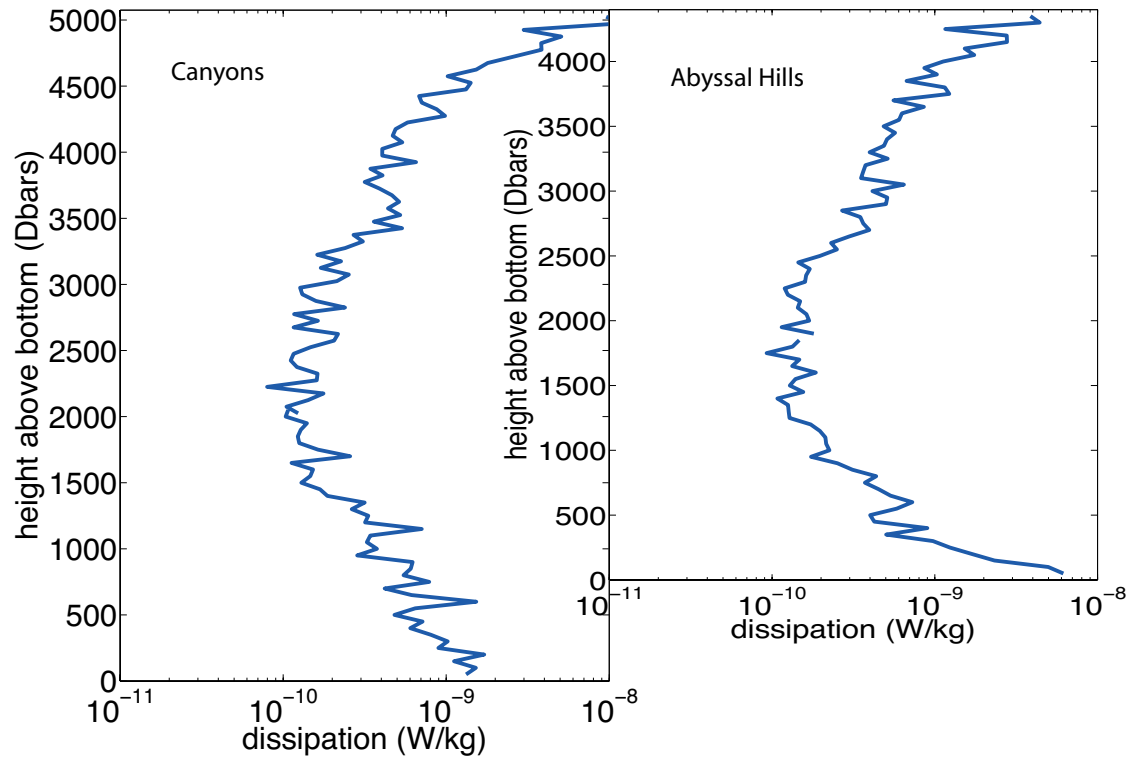


FIG. 4. Profiles of average dissipation rate ϵ vs depth for 'canyon' (left panel) and 'abyssal hill' stations. Canyon stations are represented as white filled squares and the southern most white filled circle in Figs 2&3. Abyssal hill stations are represented by the other white filled circles. The profiles have been averaged in a height-above-bottom coordinate system over the bottom most 2000 m and in a depth coordinate system in the upper part of the water column. The extent of the vertical axis represents represents the mean depth.

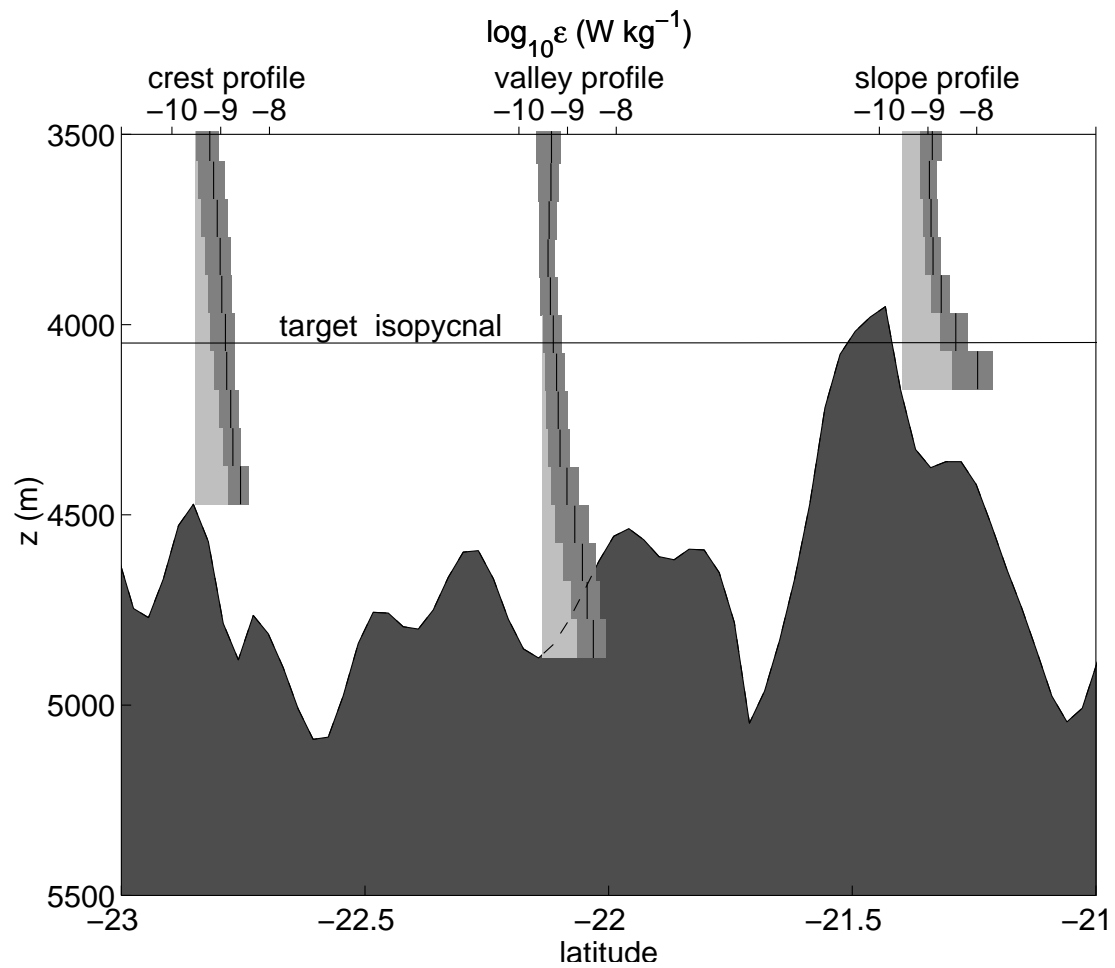


FIG. 5. Profiles of average dissipation rate ϵ vs depth for 'crest', 'valley' and 'slope' profiles, Figure from Ledwell et al. (2000), permission from *Nature*. See also Fig. 3 of St.Laurent et al. (2001).

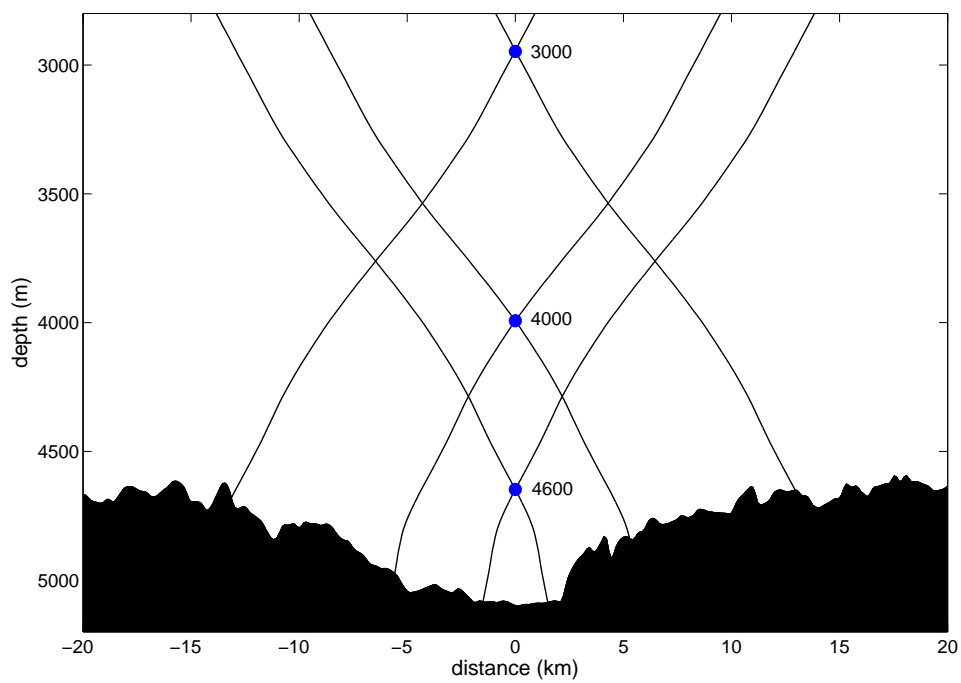


FIG. 6. Topography (black) along a line normal to the canyon axis. The origin marks the mooring position. Semidiurnal frequency rays intersecting individual current meters at nominal depths of 4600, 4000 and 3000 m are indicated. See also Fig. 2c of Toole (2007) .

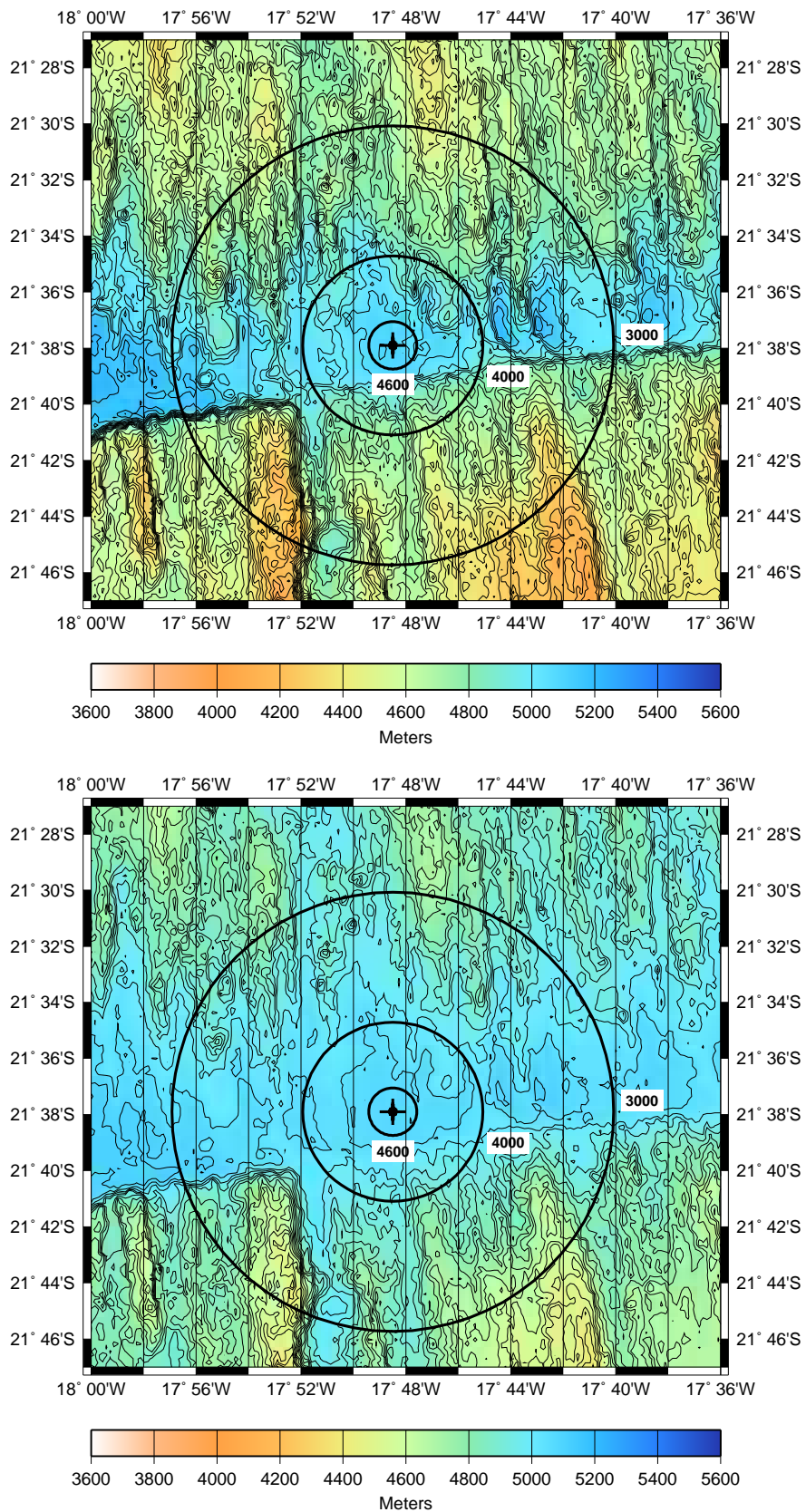


FIG. 7. 2-D multi-beam map indicating the origin of semidiurnal frequency rays passing through individual current meters. A cross marks the mooring location. Rings represent the locus of points passing through current meters at the indicated depths and originating at the depth of the mooring anchor. Upper panel: Observed bathymetry. Lower panel: Buoyancy scaled bathymetry.

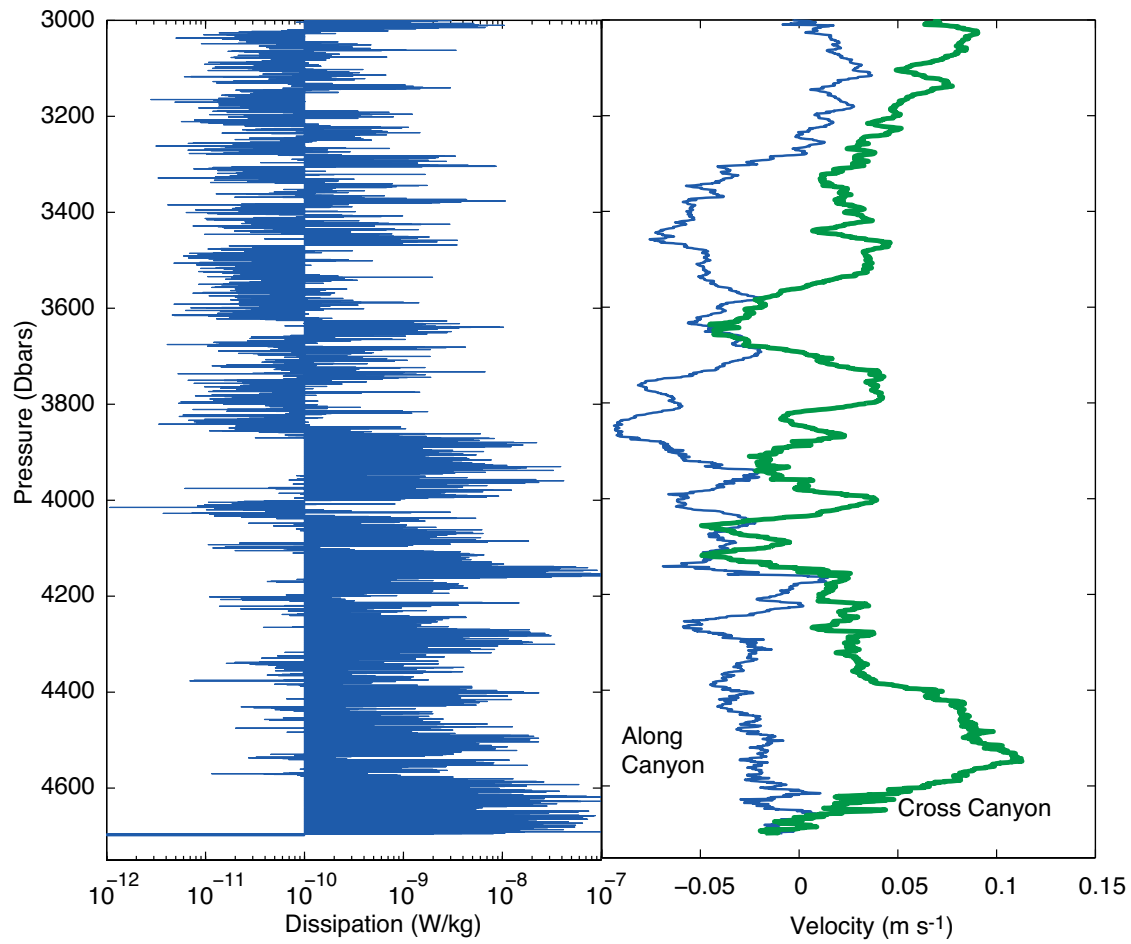


FIG. 8. Station 23 data (second Brazil Basin survey). Left panel: Dissipation. Right panel: Horizontal velocity rotated into across (thin line) and along (thick line) canyon coordinates. Variability in across-canyon velocity coincides with enhanced dissipation discussed by Thurnherr et al. (2005).